Impact of Fluid Deformation on Mixing-Induced Chemical Reactions in Heterogeneous Flows

Tanguy Le Borgne[1], Timothy Ginn[2], Marco Dentz[3]

Highlights

- Impact of fluid deformation on chemical reaction
- Reactive lamellar mixing model
- Upscaling from lamella scale to global reaction behavior

---

[1]Geosciences Rennes, UMR 6118,

Université de Rennes 1, CNRS, Rennes,

France

[2]University of California Davis, Davis,

CA, USA

[3]Spanish National Research Council,

IDAEA-CSIC, Barcelona, Spain

Fast chemical reactions in geophysical flows are controlled by fluid mixing, which perturbs local chemical equilibria and thus triggers chemical reactions. Spatial fluctuations in the flow velocity lead to deformation of material fluid elements, which form the support volumes of transported chemical species. We develop an approach based on a lamellar representation of fluid mixing that provides a direct link between fluid deformation, the distribution of concentration gradiens, and the upscaled reaction rates for fast reversible reactions. The temporal evolution of effective reaction rates are determined by the flow topology and the distribution of local velocity gradients. This leads to a significant increase of the reaction efficiency, which turns out to be orders of magnitude larger than in homogeneous flow. This approach allows for the systematic evaluation of the temporal evolution of equilibrium reaction rates, and establishes a direct link between the reaction efficiency and the spatial characteristics of the underlying flow field as quantified by the deformation of material fluid elements.

1. Introduction

Flow heterogeneity leads to chemical reaction dynamics that are very different from the ones observed under homogeneous conditions. Hence, the quantitative relation between the heterogeneity controls of mixing and effective reaction rates is of central concern in disciplines as diverse as geophysics, chemical engineering, biology and hydrology [e.g. *Tel et al.*, 2005; *Neufeld and Hernandez-Garica*, 2010; *Weiss and Provenzale*, 2008; *Dentz et al.*, 2011]. In porous media flows, effective reaction rates have been shown to differ significantly from those predicted by effective dispersion coefficients [e.g. *Gramling et al.*, 2002; *Luo et al.*, 2008; *Battiato et al.*, 2009; *Tartakovsky et al.*, 2009; *Chiogna et al.*, 2012; *de Anna et al.*, 2014a; *Hochstettler and Kitanidis*, 2013]. Geochemical reaction kinetics can be either limited by the characteristic time of intrinsic chemical phenomena (kinetic limitation) or by the time necessary to bring reactants into contact, either in solution or in the solid phase (mixing limitation).

The upscaling of kinetically limited geochemical reactions in the presence of physical and chemical medium heterogeneity has been addressed in the literature using volume averaging techniques, probability density function (PDF) approaches for the concentration statistics, multicontinuum approaches as well as reactive streamtube models [e.g., *Dentz et al.*, 2011, and literature therein]. The upscaling of mixing limited geochemical reactions, on the other hand, is still largely an open question and remains a challenge due to the intimate coupling of chemical reaction, mixing and physical heterogeneity. Recent approaches have sought to link effective reactivity to transport at local scales using particle-based Lagrangian modeling frameworks [*Tartakovsky et al.*, 2008; *Benson and*

Meerschaert, 2008; *Edery et al.*, 2009], as well as interface deformation models [*de Anna et al.*, 2014b]. Many of these works focus on irreversible homogeneous bimolecular reactions, which depend mainly on the collocation of the dissolved chemical species. Here we focus on reversible chemical reactions, such as dissolution or precipitation processes, which are triggered by the perturbation of local chemical equilibria due to fluid mixing [*De Simoni et al.*, 2005, 2007]. To date, the explicit relation between flow heterogeneity and mixing induced chemical reactions remains a key challenge, despite its importance in controlling many geochemical processes.

In this study, we start from the observation that the deformation action of heterogeneous flow fields creates a lamellar structure of the spatial distribution of the chemical species [*Duplat and Villermaux*, 2008; *Villermaux*, 2012; *Le Borgne et al.*, 2013; *de Anna et al.*, 2014b]. Geochemical transformation processes can be linked to the kinematics of mixing by focusing on the deformation of the material fluid elements, called lamellae, which form the support volumes of the heterogeneous species distributions. Note that lamella based approaches have been used for the efficient modeling of different classes of homogeneous reactions in fluctuating fluid flows [*Ranz*, 1979; *Clifford et al.*, 1998; *Clifford*, 1999]. Here we develop a reactive lamella model for reversible heterogeneous reactions that provides an explicit relation between fluid deformation and effective reaction rates. This approach is used to analyze a series of practically relevant porous media flow scenarios that exhibit distinct topological features, and quantify their impact on the temporal evolution of chemical reactivity.

2. Lamellar Mixing and Reaction

To study the fundamental interactions between fluid mixing and chemical reaction we consider the paradigmatic reversible heterogeneous reaction

$$A + B \rightleftharpoons C, \tag{1a}$$

in which C represents a pure-phase mineral and therefore has activity 1. The mass action law relates the equilibrium concentrations of A and B by $c_A c_B = K$ with K the equilibrium constant. This reaction may represent for instance mixing induced precipitation of gypsum. While simple, it captures the essence of the impact of fluid mixing on reaction systems in local chemical equilibrium [*De Simoni et al.*, 2005]. The method developed in the following can be extended straightforwardly to more complex chemical reaction systems [*De Simoni et al.*, 2007].

Transport of the dissolved species A and B is described by the advection-dispersion reaction equation

$$\frac{\partial c_i}{\partial t} + \nabla \cdot \mathbf{v} c_i - D\nabla^2 c_i = r, \tag{1b}$$

with $i = A, B$. We set the constant porosity equal to 1, which is equivalent to rescaling time. Notice that we adopt an approximate model of dispersion that relies on a constant dispersion coefficient D, in order to expedite the overall concept, and emphasize the impact of flow heterogeneity on the reaction efficiency, which is quantified by the reaction rate r. Furthermore, we assume that the dispersion coefficients are equal for both species. The methodology can be straightforwardly extended to account for anisotropic local scale dispersion. For fast reactions, the reaction rate is determined by the mixing properties of the flow and transport system. While the reaction is locally at equilibrium at each point

of the medium, this equilibrium is disturbed due to spatial mass transfer by advection and diffusion, or in other words, by mixing. Thus, the effective reaction rate depends fully on the mass transfer rates induced by the deformation of material interfaces and diffusion.

The quantitative relation between the effective reaction rate and the mixing dynamics for fast reversible chemical reaction has been studied in the papers by *De Simoni et al.* [2005, 2007]. These authors demonstrate that the reaction rate can be written as

$$r = \frac{d^2 c_i}{du^2} D(\nabla u)^2 \tag{1c}$$

where $u = c_A - c_B$ is the conservative component, (as used in conventional speciation calculations) for the bimolecular reaction, which is transported according to (1b) for $r = 0$. The mixing dynamics are encoded in the scalar dissipation rate $\chi = D(\nabla u)^2$, which reflects the elementary mass transfer mechanisms; the creation of concentration gradients and their attenuation by diffusion. Note that the form (1c) of the reaction rate requires that the diffusion coefficients for both species are equal.

2.1. The Lamellar Representation of Mixing

As solutes are transported in heterogeneous flow fields, they tend to organize into elongated structures that are naturally formed by the repeated action of advection [*Villermaux*, 2012; *Le Borgne et al.*, 2013; *de Anna et al.*, 2014b]. This is illustrated in Figure 1, where the shear action of a stratified flow field induces a deformation of the reactive fronts that may be viewed as a collection of stretched lamellae. The lamellar representation provides a powerful approach to quantify the impact of fluid deformation on mixing [*Ranz*, 1979; *Duplat and Villermaux*, 2008]. In the following, we develop an approach based on this concept to quantify the impact of these mechanisms on fast reversible reactions.

We consider solute transport in the coordinate system attached to a material segment. In this coordinate system, the flow velocity is represented by its linearization about the center of the lamella, such that $\mathbf{v}' = \boldsymbol{\epsilon} \cdot \mathbf{x}'$, where $\boldsymbol{\epsilon} = \nabla' \mathbf{v}'^T$ is the velocity gradient in the moving lamella system; the superscript T denotes the transpose. The dominant deformation is stretching along and compression perpendicular to the lamella expressed by the diagonal components ϵ_{ii}, which satisfy $\sum_i \epsilon_{ii} = 0$ due to fluid incompressibility. The relative lamella elongation is $\rho = \ell/\ell_0$ with ℓ the current and ℓ_0 the initial lamella length. Thus, the stretching rate $\epsilon_{11} = \gamma$ is given by the relative elongation ρ of the lamella as

$$\gamma = \frac{1}{\rho} \frac{d\rho}{dt}. \tag{2}$$

Thus, the evolution of concentration across the lamella satisfies [*Ranz*, 1979; *Meunier and Villermaux*, 2010]

$$\frac{\partial c_i}{\partial t} - \gamma(t) n \frac{\partial c_i}{\partial n} - D \frac{\partial^2 c_i}{\partial n^2} = r(t), \tag{3}$$

where n is the coordinate perpendicular to the main direction of elongation of the lamella, D is the local diffusion coefficient for mass transfer in the n direction exclusively. Concentration gradients in the stretching direction are much smaller than the ones perpendicular to the lamella and are ignored here. Concentration gradients in the direction perpendicular to the lamella are steepened due to compression. The width s of the lamella is a measure for the concentration gradient scale.

Notice that this picture of lamellar transport is valid as long as the lamellae can be considered as independent. This is the case for linear shear flows and radial flow scenarios, for example. In heterogeneous flows, lamellae may start interacting through co-

alescence [*Villermaux*, 2012; *Le Borgne et al.*, 2013]. The time scale for the transition from the stretching enhanced mixing regime to coalescence is typically set by the mixing time scale τ_m [*Villermaux*, 2012], which quantifies the competition of fluid deformation to decrease the lamella width and diffusion to increase it.

2.2. Dispersion and Reaction at the Lamella Scale

Equation (3) can be transformed into a diffusion-reaction equation with constant parameters by considering the variable transform [*Ranz*, 1979; *Meunier and Villermaux*, 2010] to the reduced coordinate $\tilde{n}$ and warped time τ, which are defined by

$$\tilde{n} = \frac{n}{s_0}\rho, \qquad \tau = \int_0^t dt' D\frac{\rho^2}{s_0^2} \tag{4}$$

where s_0 is the initial lamella width in the n-direction. This transformation leads to the following reaction diffusion equation:

$$\frac{\partial \tilde{c}_i}{\partial \tau} - \frac{\partial^2 \tilde{c}_i}{\partial \tilde{n}^2} = \tilde{r}(\tilde{n}, \tau), \tag{5}$$

where the concentrations $c_i(n,t)$ and the reaction rate $r(n,t)$ are related to $\tilde{c}_i(\tilde{n},\tau)$ and $\tilde{r}(\tilde{n},\tau)$ as

$$c_i(n,t) = \tilde{c}_i[\tilde{n}(n), \tau(t)] \qquad r(n,t) = \frac{D\rho^2}{s_0^2}\tilde{r}[\tilde{n}(n), \tau(t)]. \tag{6}$$

Notice that this variable transform is equivalent to a transformation into the characteristic system of (3). Notice also, that the transformation (6) assumes constant and isotropic dispersion coefficient.

The reaction rate $r(n,t)$ integrated over a lamella segment is given by

$$R_\ell(t) = \ell_0\rho \int_{-\infty}^{\infty} dn r(n,t) = \frac{D\ell_0\rho^2}{s_0} \int_{-\infty}^{\infty} d\tilde{n}\tilde{r}[\tilde{n}, \tau(t)], \tag{7}$$

where we used (4) and (6). This equation relates the reaction rate of a lamella to that of a one-dimensional diffusion-reaction system. The global, upscaled reaction rate then is given by the sum of the contributions of the individual lamellae as

$$R(t) = \sum_{\ell} R_{\ell}(t). \tag{8}$$

2.3. Fast Reversible Bimolecular Reactions

We illustrate this approach for the fast reversible bimolecular reaction system (1), which is fully determined by the mixing properties of the flow and transport system. In the coordinate system attached to the material strip, the conservative component $u = c_A - c_B$ now satisfies the diffusion equation in reduced coordinates

$$\frac{\partial u}{\partial \tau} - \frac{\partial^2 u}{\partial \tilde{n}^2} = 0. \tag{9}$$

The general expression (1c) for the reaction rate is now given in reduced coordinates by

$$\tilde{r}(\tilde{n}, \tau) = \frac{d^2 \tilde{c}_A}{du^2} \left(\frac{\partial u}{\partial \tilde{n}} \right)^2. \tag{10}$$

The concentration of species A in terms of u is obtained from the mass action law $\tilde{c}_A \tilde{c}_B = K$ and $u = \tilde{c}_A - \tilde{c}_B$ as

$$\tilde{c}_A(u) = \frac{u}{2} + \sqrt{\frac{u^2}{4} + K}. \tag{11}$$

In the following, we solve the mixing-induced reactive transport problem for a reaction front in a spatially variable flow.

2.4. Reaction Front

We consider the scenario of miscible displacement of solutions of two different chemical compositions, each at chemical equilibrium. Between the two solutions, a mixing

interface develops, that is deformed due to velocity gradients. Mass transport across the interface is, as outlined above, determined by the interaction of interface compression and diffusion/dispersion. This scenario can be described by the initial distribution $u(\tilde{n}, \tau = 0) = \frac{1}{2}\Delta u_0 \mathrm{erfc}(\tilde{n}/\sqrt{2}) + u_r$, where $\Delta u_0 = u_d - u_r$, and u_d and u_r the differences of the species concentrations in the displacing and resident fluids. As boundary conditions we set $u(-\infty, \tau) = u_d$ and $u(\infty, \tau) = u_r$. Under these conditions, the scalar distribution and the scalar gradient across the front have the scaling form

$$u(\tilde{n}, \tau) = \hat{u}(\tilde{n}/\tilde{s}), \qquad \frac{\partial u}{\partial \tilde{n}} = \frac{1}{\tilde{s}} \left. \frac{\partial \hat{u}(a)}{\partial a} \right|_{a=\tilde{n}/\tilde{s}}, \tag{12}$$

where we defined the non-dimensional interface width $\tilde{s} = \sqrt{1 + 2\tau}$. The scaling function here is simply given by $\hat{u}(\tilde{n}) = u(\tilde{n}, 0)$. Using the scaling forms (12) in (10), we obtain for the global reaction rate (7) on a single lamella the expression

$$R_\ell = \frac{\ell_0 s_0 \Delta u_0 \mathcal{A} s_0 \rho^2}{\tau_D \sqrt{1 + 2\tau}}, \tag{13}$$

where the constant $\mathcal{A}$ is given by

$$\mathcal{A} = \frac{1}{\Delta u_0} \int_{-\infty}^{\infty} da \frac{d^2 c_A}{d\hat{u}^2} \left(\frac{\partial \hat{u}}{\partial a} \right)^2. \tag{14}$$

The diffusion time τ_D over the initial interface width is given by $\tau_D = s_0^2/D$. The solution (13) aligns clearly the terms contributing to the global reaction rate: diffusion quantified by D, lamella elongation and elongation history through warped time τ, see (4), and the speciation term encoded in $\mathcal{A}$, which represents the chemistry. This general result shows that for a single fast reaction the effective rate when mixing limited is dependent on the nature of the chemical equilibrium and on the entire history of the deformation of the individual lamellae making up the mixing front. In principle this means that given

a deterministic, or suitable stochastic, definition of the deformation paths taken by the lamellae making the front, the global reaction rate can be computed, for essentially arbitrary nonuniform flows and heterogeneous flows in general.

The reactive transport scenario is illustrated in Figure 1 for a heterogeneous stratified flow. To quantify the reaction dynamics at the diffuse interface, the front is considered as a set of lamellae, on which chemical gradients develop and reactions occur.

3. Stretching Scenarios and Reaction Rates

We evaluate the impact of stretching enhanced mixing as quantified by the global reaction rate (13) for a series of idealized yet fundamental stretching scenarios that exhibit distinct topological features. We study these basic cases to test the theoretical results of Section 2 and to provide a basis for subsequent analyses of more sophisticated case studies. Uniform homogeneous flow serves as the base case, then we consider a radial flow scenario as well as linear and random shear flows.

3.1. Uniform Homogeneous Flow

Under uniform homogeneous flow conditions, there are no velocity gradients and therefore there is no deformation of material fluid elements. Thus, relative elongation is constant $\rho = 1$ and warped time is simply time rescaled by τ_D as $\tau = \frac{t}{\tau_D}$. This gives for the global reaction rate the simple expression

$$R(t) = \frac{L s_0 \Delta u_0 A}{\tau_D \sqrt{1 + 2\frac{t}{\tau_D}}}, \tag{15}$$

where L is the initial front length. For times $t \ll \tau_D$ diffusion has not smoothed the concentration gradient at the interface, which is nearly constant, while mass is transferred

across the interface at constant rate. Thus, the reaction rate is approximately constant. For times $t \gg \tau_D$, concentration gradients decrease due to diffusive interface growth and thus the reaction rate decreases as $t^{-1/2}$.

3.2. Radial Flow

We now consider a reaction front under radial flow conditions, which is typical of field operations for pump and treat groundwater remediation, geothermal energy exploitation and carbon dioxide storage in deep saline aquifers [e.g., *Kitanidis and McCarthy*, 2012; *Nordbotten and Celia*, 2012].

For a constant volumetric flow rate Q at the well, the radial flow velocity is given by $v(r) = Q/(2\pi r h)$ for $r > r_w$ with r_w the well radius. Mass conservation gives for the front radius $r_f(t) = r_w\sqrt{\alpha t + 1}$ where the strain rate $\alpha = Q/(\pi r_w^2 h)$ with h the height of the flow domain (e.g. confined aquifer or fracture). The relative front length $\rho = r_f/r_w$ then is given by $\rho = \sqrt{\alpha t + 1}$. Thus, we obtain for the warped time τ

$$\tau = \frac{t}{\tau_D}\left(1 + \frac{\alpha t}{2}\right). \tag{16}$$

From (13), the global reaction rate then is given by

$$R = \frac{L s_0 h \Delta u_0 \mathcal{A}}{\tau_D} \frac{\alpha t + 1}{\sqrt{1 + 2\frac{t}{\tau_D}\left(1 + \frac{\alpha t}{2}\right)}}, \tag{17}$$

where $L = 2\pi r_w$. For times $\alpha^{-1} \ll t \ll \tau_m$, the reaction rate increases linearly with time as

$$R = \frac{L s_0 \ell_0 h \Delta u_0 \mathcal{A}}{\tau_D} \alpha t, \tag{18}$$

as a result of stretching enhanced mass transfer across the interface and the $\sqrt{t}$ evolution of the interface length. The mixing time here is given by $\tau_m = \sqrt{\tau_D/\alpha}$. For $t \gg \tau_m$ the

reaction converges towards the constant

$$R = Ls_0 h \Delta u_0 \mathcal{A} \sqrt{\frac{\alpha}{2\tau_D}} \tag{19}$$

which reflects the balance between the increases of the interface length as $\sqrt{t}$ and diffusive mass transfer across it as $1/\sqrt{t}$. It is worth pointing out that this has implications for the evaluation of reactive push-pull tracer tests [*Istok*, 2013] because reactivity is enhanced by the mere deformation of the radial solute interface.

3.3. Linear Shear Flow

Here we consider the impact of linear shear deformation on chemical reactions. This type of flow topology is realized locally in heterogeneous $d = 2$ dimensional media where the Okubo-Weiss parameter, or equivalently, the determinant of the velocity gradient is equal to zero [*Okubo*, 1970; *Weiss and Provenzale*, 2008]. Linear shear flows are naturally realized in double diffusion experiments between salt and freshwater [*Dror et al.*, 2003a, b], and may occur for saltwater intrusion in coastal aquifers at low Péclet numbers [*Dentz et al.*, 2006]. *Bolster et al.* [2011] studied the shear and stretching enhanced mixing of a conservative solute in this type of flow field.

The flow field is given by $\mathbf{v}(y) = \sigma y \mathbf{e}_1$ aligned with the 1–direction of the coordinate system, σ is the shear rate. The interface is aligned perpendicular to the direction of stratification such that the relative lamella elongation is given by $\rho = \sqrt{1 + (\sigma t)^2}$. Accordingly, we obtain for the warped time τ

$$\tau = \frac{t}{\tau_D} \left[1 + \frac{(\sigma t)^2}{3} \right]. \tag{20}$$

Hence, we obtain from (13) for the global reaction rate

$$R = \frac{Ls_0\Delta u_0\mathcal{A}}{\tau_D}\frac{1+(\sigma t)^2}{\sqrt{1+2\frac{t}{\tau_D}\left[1+\frac{(\sigma t)^2}{3}\right]}}. \tag{21}$$

For $\sigma^{-1} \ll t \ll \tau_m$, it increases quadratically with time as

$$R \approx \frac{Ls_0\Delta u_0\mathcal{A}}{\tau_D}(\sigma t)^2. \tag{22}$$

The mixing time scale $\tau_m = (\tau_D/\sigma^2)^{1/3}$ denotes the time at which the compression deformation of the line due to shear equilibrates with diffusion [*Villermaux*, 2012; *Le Borgne et al.*, 2013]. The significant increase in the global reaction rate is due to the linear evolution of the interface length on one hand and stretching enhanced mass transfer on the other. For $t \gg \tau_m$, the reaction rate approaches asymptotically

$$R = Ls_0\Delta u_0\mathcal{A}|\sigma|\sqrt{\frac{3t}{2\tau_D}}. \tag{23}$$

This behavior is the result of the linear interface elongation combined with essentially diffusive mass transfer across the interface. In both regimes, the reaction rate is dramatically increased compared to the case of uniform homogeneous flow. Figure 2 shows the evolution of the global reaction rates for linear shear, radial and uniform flow.

3.4. Stratified Random Flow

Transport in stratified random flow [*Matheron and de Marsily*, 1980] has been frequently studied in the literature as a model for heterogeneous aquifers [*Zavala-Sanchez et al.*, 2009, and literature therein]. In fact, many geological media exhibit geostatistical stratification, which means that the horizontal correlation length is much larger than the vertical. Random shear flow both steady and unsteady have been studied in the physics literature as

a simplified model for heterogenous and turbulent flows [*Bouchaud and Georges*, 1990; *Majda and Kramer*, 1999].

We consider the random shear flow $\mathbf{v}(y) = v(y)\mathbf{e}_1$ aligned with the 1–direction of the coordinate system. A material fluid segment initially located at $x = 0$ and $y = y_0$ is elongated according to

$$\rho = \sqrt{\sigma(y_0)^2 t^2 + 1}, \tag{24}$$

The shear rate is given by $\sigma(y_0) = [v(y_0 + \ell_0) - v(y_0)]/\ell_0$ with ℓ_0 the initial lamella size, which is much smaller than the variation scale of the shear rate. The reaction rate for a single lamella is given by (21) with $\sigma \equiv \sigma(y_0)$. The global reaction rate is obtained by integration over the PDF $p_\sigma(\sigma)$ of shear rates and multiplication by the number of lamellae L/ℓ_0 such that

$$R = Ls_0\Delta u_0 \mathcal{A} \int_{-\infty}^{\infty} d\sigma \frac{p_\sigma(\sigma)[1 + (\sigma t)^2]}{\tau_D \sqrt{1 + 2\frac{t}{\tau_D}\left[1 + \frac{(\sigma t)^2}{3}\right]}}. \tag{25}$$

where L is the initial front length. The PDF $p_\sigma(\sigma)$ is obtained by spatial sampling along the initial line of length L as

$$p_\sigma(\sigma) = \frac{1}{L}\int_0^L dy_0 \delta_{\ell_0}[\sigma - \sigma(y_0)], \tag{26}$$

where $\delta_{\ell_0}(\sigma)$ is a sampling function of width ℓ_0 and height $1/\ell_0$.

At times $t \ll \tau_m$, the global reaction rate (25) behaves as

$$R \approx \frac{Ls_0\Delta u_0 \mathcal{A}}{\tau_D}\langle\sigma^2\rangle t^2. \tag{27}$$

where the angular brackets denote the average over the distribution of shear rates. The mixing time here is set by the average absolute shear rate as $\tau_m = (\tau_D/\langle|\sigma|\rangle^2)^{1/3}$. In this

early time regime, the reaction rate is related to the mean squared shear rate if it exists. For times $t \gg \tau_m$, we obtain the characteristic $t^{1/2}$ behavior

$$R = Ls_0 \Delta u_0 \mathcal{A} \langle |\sigma| \rangle \sqrt{\frac{3t}{2\tau_D}}. \tag{28}$$

Notice that in this regime, the reaction rate is quantified in terms of the mean absolute shear rate. To illustrate the impact of the shear rate distribution on the reaction behavior, we consider now a distribution with well defined variance, and a broad distribution of shear rates for which the variance does not exist.

Thus, we employ the Gaussian distribution $p_\sigma(\sigma) = \exp[-\sigma^2/(2\langle\sigma^2\rangle)]/\sqrt{2\pi\langle\sigma\rangle^2}$. The mean absolute shear rate here is $\langle|\sigma|\rangle = \sqrt{2\langle\sigma^2\rangle/\pi}$. In order to illustrate the reaction behavior for a broad distribution of shear rates, we consider a shear rate that follows the distribution $p_\sigma = \beta\sigma_0^{-1}(1+\sigma/\sigma_0)^{-1-\beta}$ for $\sigma > 0$ and $1 < \beta < 2$. The mean shear rate is given by $\langle\sigma\rangle = \sigma_0/(\beta-1)$, the variance is not defined.

Figure 3 shows the behavior of the global reaction rate for a constant shear rate, the Gaussian and the power-law distribution. The behaviors for the constant shear rate and the Gaussian shear distribution are almost identical. This is no surprise as the early and late time behaviors are determined by the variance and mean absolute shear rate, respectively. The reaction rate for the power-law shear distribution shows a different behavior at short times, which can be traced back to the fact that the variance of shear rates is not defined here. In fact, with the same mean shear rate, the power-law distribution provides a much broader spectrum of shears (towards high shear) than the Gaussian distribution, which leads to an overall increased reaction rate.

4. Conclusions

We quantify the impact of fluid deformation on mixing-induced reversible reactions in heterogeneous flows using an approach that treats the reactive mixture as a composition of individual lamellae. This is achieved by bridging the way that different flow topological features impact solute mixing [e.g. *De Barros et al.*, 2012; *Le Borgne et al.*, 2013] with the role of the scalar dissipation rate in effective kinetics of mixing-controlled reactions [e.g. *De Simoni et al.*, 2005, 2007], through equation (13). This representation reduces much of the complexity while honoring the mixing on the lamella as it is transported and deformed in the heterogeneous flow. It is valid as long as the lamella can be considered as independent. For heterogeneous flows this means before the mixing time, which is set by the interaction of flow deformation and dispersion. The approach, illustrated here by a bimolecular reaction involving two dissolved species and a mineral phase, may be extended to a range of mixing-driven geochemical reactions characterized by more complex reaction networks.

We derive an explicit expression for the lamella scale reaction rate that deciphers the roles of fluid deformation, dispersion and chemical reaction. The global reaction rate is obtained from the sum of the contributions of individual lamellae and thus integrates the heterogeneous distribution of velocity gradients into large scale reactivity. We demonstrate that the upscaled reaction rate (per Eq. 13) depends explicitly on the history of lamellae deformation related to the distribution of local velocity gradients. The derived approach is illustrated through the analysis of four simplified yet fundamental reactive flow scenarios characterized by distinct topological features. Note that flows in natu-

ral heterogeneous media show in general more complex stretching behaviors than these idealized flow fields [*Le Borgne et al.*, 2013], which, however, can be straightforwardly incorporated in the developed methodology through a statistical description of lamellar stretching.

This approach opens an avenue to the long-standing problem of upscaling mixing-driven reactive transport because it accommodates non-linear transformations in heterogeneous mixtures via a statistical description of the lamellae kinematics, which can in principle be derived from the flow heterogeneity.

Acknowledgments. Data used for producing the figures can be obtained by solving the respective equations given in the manuscript. MD acknowledges the support of the European Research Council (ERC) through the project MHetScale (617511).

References

Battiato, I., D. M. Tartakovsky, A. M. Tartakovsky, and T. Scheibe (2009), On breakdown of macroscopic models of mixing-controlled heterogeneous reactions in porous media, *Adv. Water Resour.*, *32*(11).

Benson, D. A., and M. M. Meerschaert (2008), Simulation of chemical reaction via particle tracking: Diffusion-limited versus thermodynamic rate-limited regimes, *Water Resour. Res.*, *44*, W12,201.

Bolster, D., M. Dentz, and T. Le Borgne (2011), Hyper mixing in shear flow, *Water Resour. Res.*, *47*, W09,602.

Bouchaud, J. P., and A. Georges (1990), Anomalous diffusion in disordered media: Statistical mechanisms, models and physical applications, *Phys. Rep.*, *195*(4,5), 127–293.

Chiogna, G., D. Hochstetler, A. Bellin, P. Kitanidis, and M. Rolle (2012), Mixing, entropy and reactive solute transport, *Geophys. Res. Lett.*, *30*, L20,405.

Clifford, M. J. (1999), A Gaussian model for reaction and diffusion in a lamellar structures, *Chem. Eng. J.*, *54*, 303–310.

Clifford, M. J., S. M. Cox, and E. P. L. Roberts (1998), Lamellar modelling of reaction, diffusion and mixing in a two-dimensional flow, *Chem. Eng. Sci.*, *71*, 49–56.

de Anna, P., J. Jimenez-Martinez, H. Tabuteau, R. Turuban, T. Le Borgne, M. Derrien, and Y. Méheust (2014a), Mixing and reaction kinetics in porous media: An experimental pore scale quantification, *Environ. Sci. Technol.*, *48*(508-516), 508516.

de Anna, P., M. Dentz, A. Tartakovsky, and T. Le Borgne (2014b), The filamentary structure of mixing fronts and its control on reaction kinetics in porous media flows, *Geophys. Res. Lett.*, *41*, 45864593.

De Barros, F., M. Dentz, J. Koch, and W. Nowak (2012), Flow topology and scalar mixing in spatially heterogeneous flow fields, *Geophys. Res. Lett.*, *39*, L08,404.

De Simoni, M., J. Carrera, X. Sánchez-Vila, and A. Guadagnini (2005), A procedure for the solution of multicomponent reactive transport problems, *Water Resour. Res.*, *41*, 2005WR004,056.

De Simoni, M., X. Sanchez-Vila, J. Carrera, and M. Saaltink (2007), A mixing ratios-based formulation for multicomponent reactive transport, *Water Resour. Res.*, *43*, W07,419.

Dentz, M., D. M. Tartakovsky, E. Abarca, A. Guadagnini, X. Sanchez-Vila, and J. Carrera (2006), Variable density flow in porous media, *J. Fluid Mech.*, *561*, 209–235.

Dentz, M., T. LeBorgne, A. Englert, and B. Bijeljic (2011), Mixing, spreading and reaction in heterogeneous media: A brief review, *J. Cont. Hydrol.*, *120-121*, 1–17, doi: 10.1016/j.jconhyd.2010.05.002.

Dror, I., T. Amitay, B. Yaron, and B. Berkowitz (2003a), Salt-pump mechanism for contaminant intrusion into coastal aquifers, *Science*, *300*, 5621.

Dror, I., B. Yaron, and B. Berkowitz (2003b), Response to comment on Salt-pump mechanism for contaminant intrusion into coastal aquifers, *Science*, *302*, 5646.

Duplat, J., and E. Villermaux (2008), Mixing by random stirring in confined mixtures, *Journal of Fluid Mechanics*, *617*, 51, doi:10.1017/S0022112008003789.

Edery, Y., H. Scher, and B. Berkowitz (2009), Modeling bimolecular reactions and transport in porous media, *Geophysical Research Letters*, *36*(2), 1–5, doi: 10.1029/2008GL036381.

Gramling, C. M., C. F. Harvey, and L. C. Meigs (2002), Reactive transport in porous media: A comparison of model prediction with laboratory visualization, *Environ. Sci. Technol.*, *36*, 2508 – 2514.

Hochstettler, D. L., and P. K. Kitanidis (2013), The behavior of effective reaction rate constants for bimolecular reaction under physical equilibrium, *J. Contam. Hydrol.*, *144*, 88–98.

Istok, J. D. (2013), *Push-Pull Tests for Site Characterization*, Springer Heidelberg New York.

Kitanidis, P. K., and P. L. McCarthy (2012), *Delivery and Mixing in the Subsurface: Processes and Design Principles for In Situ Remediation*, Springer.

Le Borgne, T., M. Dentz, and E. Villermaux (2013), Stretching, coalescence and mixing in porous media, *Phys. Rev. Lett.*, *110*, 204,501.

Luo, J., M. Dentz, J. Carrera, and P. Kitanidis (2008), Effective reaction parameters for mixing controlled reactions in heterogeneous media, *Water Resour. Res.*, *44*, W02,416.

Majda, A. J., and P. R. Kramer (1999), Simplifed models for turbulent difusion: Theory, numerical modelling, and physical phenomena, *Phys. Rep.*, *314*, 237–574.

Matheron, M., and G. de Marsily (1980), Is transport in porous media always diffusive?, *Water Resour. Res.*, *16*, 901–917.

Meunier, P., and E. Villermaux (2010), The diffusive strip method for scalar mixing in two dimensions, *J. Fluid Mech.*, *662*, 134–172.

Neufeld, Z., and E. Hernandez-Garica (2010), *Chemical and Biological Processes in Fluid Flows: A dynamical System Approach*, Imperial College Press, London.

Nordbotten, J. M., and M. A. Celia (2012), *Geological Storage of CO_2*, Wiley.

Okubo, A. (1970), Horizontal dispersion of floatable particles in the vicinity of velocity singularities such as convergences, *Deep-Sea Res.*, *17*, 445–454.

Ranz, W. E. (1979), Application of a stretch model to mixing, diffusion and reaction in laminar and turbulent flows, *AIChE Journal*, *25*(1), 41–47.

Tartakovsky, A. M., D. M. Tartakovsky, and P. Meakin (2008), Stochastic Langevin model for flow and transport in porous media, *Phys. Rev. Lett.*, *101*(4), 044502, doi: 10.1103/PhysRevLett.101.044502.

Tartakovsky, A. M., G. D. Tartakovsky, and T. D. Scheibe (2009), Effects of incomplete mixing in multicomponent reactive transport, *Adv. in Water Res.*, *32*, 1674–1679.

Tel, T., A. Demoura, C. Grebogi, and G. Karolyi (2005), Chemical and biological activity in open flows: A dynamical system approach, *Physics Reports*, *413*(2-3), 91–196, doi: 10.1016/j.physrep.2005.01.005.

Villermaux, E. (2012), Mixing by porous media, *C. R. Mécanique*, *340*, 933–943.

Weiss, J., and A. Provenzale (2008), *Transport and Mixing in Geophysical Flows*, 744, Springer Verlag.

Zavala-Sanchez, V., M. Dentz, and X. Sanchez-Vila (2009), Characterization of mixing and spreading in a bounded stratified medium, *Adv. Water Resour.*, *32*, 635–648.

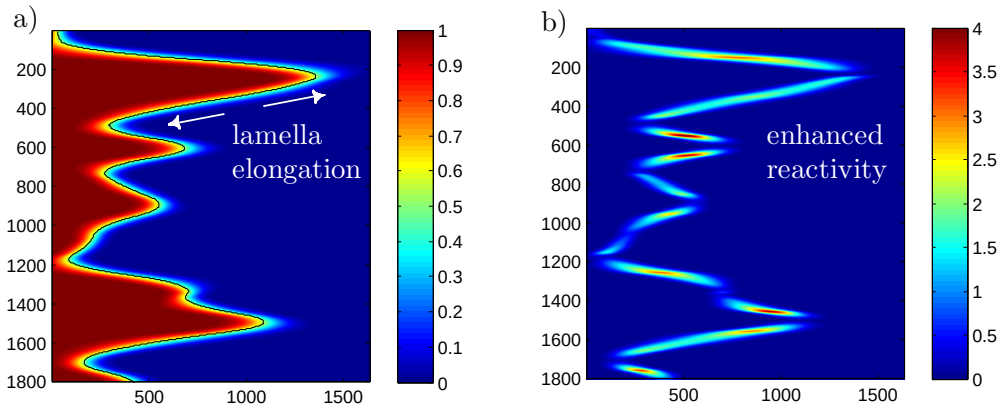

Figure 1. Illustration of a reaction front in a stratified random flow field based on lamellar mixing. (a) Concentration profile of the conservative component illustrating the interface between displacing and resident waters, which is deformed by the action of the flow heterogeneity and develops a lamellar structure. (b) Reaction rates along the interface normalized by the reaction rates for homogeneous flow. Interface elongation enhances concentration gradients by decreasing the lamella width and thus increases chemical reactivity.

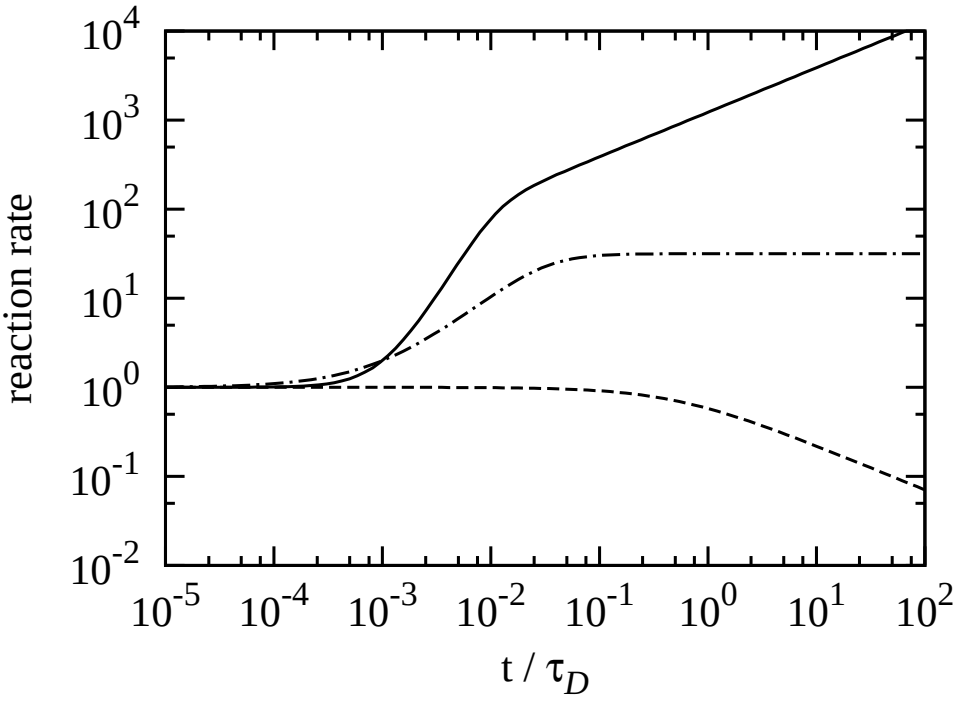

Figure 2. Global reaction rates for (solid) linear shear flow with $\sigma = 1$, (dashed-dotted) radial flow with $\alpha = 1$, and (dashed) uniform flow. The reaction rates are normalized by $Ls_0\Delta u_0\mathcal{A}/\tau_D$.

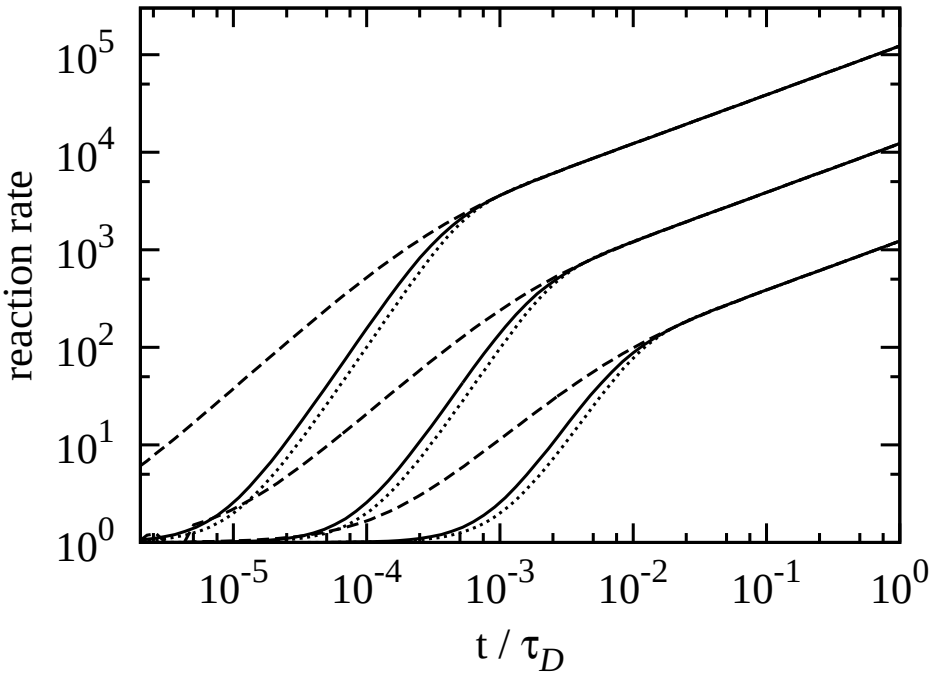

Figure 3. Global reaction rates for (solid) Gaussian distributed, (dashed) power-law ($\beta = 3/2$) distributed shear rates and (dotted) constant shear rate for (top to bottom) $\langle|\sigma|\rangle = 10^2$, 10^1 and 1. The reaction rates are normalized by $Ls_0\Delta u_0\mathcal{A}/\tau_D$.